

2

DRY DOCUMENTATION PAGE

DTIC FILE COPY

AD-A229 776

25. DECLASSIFICATION/DOWNGRADING SCHEDULE

1b. RESTRICTIVE MARKINGS

3. DISTRIBUTION/AVAILABILITY OF REPORT

Unclassified/Unlimited

4. PERFORMING ORGANIZATION REPORT NUMBER(S)
ONR Technical Report #16

5. MONITORING ORGANIZATION REPORT NUMBER(S)

5a. NAME OF PERFORMING ORGANIZATION
Dept of Chemical Engineering
and Materials Science

5b. OFFICE SYMBOL
(If applicable)
Code 11i3

7a. NAME OF MONITORING ORGANIZATION
Office of Naval Research

5c. ADDRESS (City, State, and ZIP Code)
University of Minnesota
Minneapolis, MN 55455

7b. ADDRESS (City, State, and ZIP Code)
800 North Quincy Street
Arlington, VA 22217

5a. NAME OF FUNDING/SPONSORING ORGANIZATION
Office of Naval Research

5b. OFFICE SYMBOL
(If applicable)

9. PROCUREMENT INSTRUMENT IDENTIFICATION NUMBER
Contract No. N00014-87-K-0494

5c. ADDRESS (City, State, and ZIP Code)
800 North Quincy Street
Arlington, VA 22217-5000

10. SOURCE OF FUNDING NUMBERS
PROGRAM ELEMENT NO. PROJECT NO. TASK NO. WORK UNIT ACCESSION NO.

11. TITLE (Include Security Classification)
Imaging of Stacking Faults in Highly Oriented Pyrolytic Graphite using Scanning Tunneling Microscopy

12. PERSONAL AUTHOR(S)
S. Snyder, T. Foecke, H.S. White, and W.W. Gerberich

13a. TYPE OF REPORT
Technical

13b. TIME COVERED
FROM 1/1/90 TO 10/31/90

14. DATE OF REPORT (Year, Month, Day)
12/3/90

15. PAGE COUNT
13

16. SUPPLEMENTARY NOTATION
Submitted to Applied Physics Letters, November 1990

COSATI CODES		
FIELD	GROUP	SUB-GROUP

18. SUBJECT TERMS (Continue on reverse if necessary and identify by block number)

19. ABSTRACT (Continue on reverse if necessary and identify by block number)
Scanning tunneling microscopy images of the (0001) plane of highly oriented pyrolytic graphite show defect regions consisting of an extensive network of partial dislocations that form extended and contracted nodes. The partial dislocations in hexagonal graphite enclose triangular regions (about 1000 nm on a side) of faulted material comprised of rhombohedral graphite. Tunneling spectroscopy shows differences in the dependence of the tunneling current on voltage between the faulted and unfaulted regions. Electronic and elastic interactions of the tip with the HOPG surface are proposed to explain the observed image contrast between hexagonal and rhombohedral graphite.

(772)

20. DISTRIBUTION/AVAILABILITY OF ABSTRACT
 UNCLASSIFIED/UNLIMITED SAME AS RPT DTIC USERS

21. ABSTRACT SECURITY CLASSIFICATION
Unclassified

22a. NAME OF RESPONSIBLE INDIVIDUAL
Henry S. White

22b. TELEPHONE (Include Area Code) 22c. OFFICE SYMBOL
(612) 625-6995

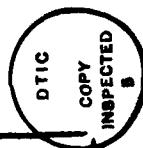
Imaging of Stacking Faults in Highly Oriented Pyrolytic Graphite using Scanning Tunneling Microscopy

S. Snyder, T. Foecke, H.S. White, and W.W. Gerberich
Department of Chemical Engineering and Materials Science
University of Minnesota
Minneapolis, MN 55455

Scanning tunneling microscopy images of the (0001) plane of highly oriented pyrolytic graphite show defect regions consisting of an extensive network of partial dislocations that form extended and contracted nodes. The partial dislocations in hexagonal graphite enclose triangular regions (~1000 nm on a side) of faulted material comprised of rhombohedral graphite. Tunneling spectroscopy shows differences in the dependence of the tunneling current on voltage between the faulted and unfaulted regions. Electronic and elastic interactions of the tip with the HOPG surface are proposed to explain the observed image contrast between hexagonal and rhombohedral graphite.

Submitted to *Applied Physics Letters*, November, 1990.

Accession For	
NTIS GRA&I	<input checked="" type="checkbox"/>
DTIC TAB	<input type="checkbox"/>
Unannounced	<input type="checkbox"/>
Justification	
By _____	
Distribution/	
Availability Codes	
Dist	Avail and/or Special
A-1	



Highly oriented pyrolytic graphite (HOPG) is used extensively as a substrate and calibration standard in scanning tunneling microscopy (STM). In spite of its wide spread use, characterization of the structural and electronic properties of graphite using STM and tunneling spectroscopy (TS) has been difficult, due in part to the crystalline disorder in commercial polycrystalline HOPG samples used for STM studies. Reports have documented unusual observations of graphite in scanning tunneling microscopy images, such as "giant corrugations"^{1,2(a)}, large tunneling current asymmetries between adjacent carbon atoms^{2(b)}, and large scale hexagonal patterns rotated at various angles with respect to the normal atomic corrugations^{3,4}. Explanations for these anomalies are still being forwarded, although no conclusive answers have been agreed upon. Here, we report an extensive triangular network found in STM images of the (0001) plane of HOPG and discuss several possible explanations for the contrast mechanism observed in these images. Comparison of the present STM images with previous transmission electron microscopy (TEM) images of HOPG allows unequivocal identification of the observed extended network as an array of alternating hexagonal and rhombohedral graphite.

Tunneling experiments were performed on a freshly cleaved sample of HOPG (grade B from Union Carbide). A commercial STM (Nanoscope II, Digital Instruments Inc.) was used to acquire constant current images and current-voltage (I-V) curves in air. STM tips were made by mechanically cutting Pt-Rh (80-20%) wire. Images reported here were recorded using a bias voltage of 30 mV (sample vs tip), a set-point current of 1.1 nA, and a scan rate of 4.34 Hz.

Figures 1(a, b) are STM images of an array of triangles on the (0001) surface of HOPG. STM images of arrays similar to these are occasionally observed in our laboratory when using HOPG as a substrate for STM studies. The defect region, which is in excess of 4000 nm x 4000 nm, begins near a crystal growth

defect at a cleavage step (lower left corner of Fig. 1(b)). The triangles increase in size with distance away from the step. The triangular shapes range from equilateral triangles to triangles where one of the corners extends into a long ribbon. Within the array, the light triangles appear displaced above the darker triangular regions by $\sim 4 \text{ \AA}$. Three triangles intersect forming a bright point, displaced by $\sim 5 \text{ \AA}$ above the surface of the dark triangles. Imaging a similar array (1000 nm x 1000 nm) (not shown) on a different HOPG sample shows that at a higher bias voltage ($\sim 400 \text{ mV}$) the contrast between the elevated triangular (light) and adjacent (dark) regions decreases to $\sim 1 \text{ \AA}$.

Triangular arrays on HOPG⁵⁻⁷ similar to those observed in Fig.1 have been observed by TEM (Fig.2). The structures observed by TEM range in size from several tenths to several micrometers on an edge, as in the STM images. In a detailed report, the diffraction contrast in the TEM images was attributed by Williamson⁵ to rhombohedral stacking faults formed as extended nodes between dissociated basal screw dislocations in the hexagonal structure. In accordance with TEM data, the lighter triangular areas in the STM images (faulted regions) in Fig.1(a, b) are assigned a rhombohedral crystal structure and the darker areas (unfaulted regions) would have a hexagonal crystal structure.

The most common form of graphite consists of a hexagonal stacking of hexagonally bonded carbon atoms. Rhombohedral graphite differs from hexagonal graphite in the atomic plane stacking (Fig. 3). Hexagonal graphite has ABABA-type stacking while rhombohedral graphite has ABCABC-type. Dislocations in HOPG are assumed to be basal screw dislocations since slip in a plane inclined to the basal plane would require the breaking of strong in-plane bonds rather than the weak van der Waals interplanar bonds. Although extensive experimentation has been performed on this material in the TEM⁵⁻⁷, slip on non-basal slip systems has not been observed. The slip observed in HOPG by TEM is generally in the form of

arrays of partial dislocations which can combine into a perfect basal dislocation following the general reaction

$$\frac{1}{3} a [10\bar{1}0] + \frac{1}{3} a [1\bar{1}00] = \frac{1}{3} a [2\bar{1}\bar{1}0]$$

These partials describe the translocation needed to convert a 'B' layer to a 'C' layer, and form the line separating the faulted and unfaulted regions, Fig. 3(c).

Considering the abovementioned properties of graphite, there are several possible explanations for the contrast observed in the STM images. One is that an actual z-displacement exists between the unfaulted and faulted regions in the array. The most obvious mechanism that may produce a triangular array is an intersecting network of slip upsets. If the assumption that slip is contained in the basal plane holds, the burgers vectors are completely contained in the basal plane, and there can be no displacement in the z-direction due to slip. Although dislocations with a burgers vector $[000c]$ in the form of sessile loops have been observed in TEM images⁶, they have generally been observed as isolated loops and do not form triangular arrays. With no prior evidence of non-basal slip, this possibility seems unlikely. A second possibility is that the apparent z-displacement could be caused by a distortion of the lattice upon formation of a stacking fault. Since the interplanar spacings of rhombohedral and hexagonal graphite are the same⁸, this could not give rise to a z-displacement.

The observed contrast in the STM images may be purely electronic in origin. Band structure calculations indicate that rhombohedral graphite is a semiconductor with a direct band gap of ~ 0.05 eV⁹. Fahy et. al. considered this calculated gap value to be an underestimate due to the local-density formalism used in the calculation⁹. In contrast, hexagonal graphite is a semimetal. Thus, rhombohedral and hexagonal will have some differences in the density of states near the Fermi level. The temperature variation of the electrical conductivity

displays a semimetallic character in pure hexagonal graphite crystals and a semiconducting character in pyrolytic graphite (which is known to contain 5-10% rhombohedral graphite)⁹. Fahy et. al. conclude this can be explained only by a difference in the band structure between the two forms of graphite⁹.

Further support for the influence of electronic effects on the image contrast comes from the discovery of superperiodic structures on the (0001) plane of HOPG^{3,4}. It has been postulated a misorientation of the second layer (and possibly the third layer) in HOPG with respect to the surface perturbs the surface density of states, causing a distortion of the tunneling characteristics from that observed in normal hexagonal HOPG. Extending the explanation of the image contrast observed in these superperiodic structures, it is probable that the difference in the position of the subsurface atoms of hexagonal and rhombohedral graphite (Fig. 3) may affect the tunneling characteristics of the faulted and unfaulted regions.

An additional mechanism which may enhance the image contrast involves the elastic interaction of the tip with the sample surface. Giant atomic corrugations with an amplitude of up to 24 Å have been observed on HOPG^{2(a)}. It has been theorized that the STM tip elastically deforms the surface of HOPG upon scanning¹ causing corrugation amplitudes larger than expected on the basis of electronic effects alone. In addition, reflection electron microscopy (REM) accomplished during STM imaging on graphite have shown elastic deflections of the surface¹⁰ as the tip passed over the surface. Assuming a difference in the elastic moduli of the two crystal structures of graphite, the elastic deflections induced by the tip during scanning would have a different magnitude causing a difference in the measured z-displacement in STM images. However, we are not aware of measurements of the elastic modulus of rhombohedral graphite, therefore a direct comparison between theory and experimental results is not presently possible.

Preliminary TS measurements were performed in the defect region. Current-voltage, (I-V), curves (Fig. 4) obtained over an elevated triangular region (curve A, rhombohedral) and adjacent region (curve B, hexagonal) reproducibly show a factor of two difference in the magnitude of the tunneling current (constant tip to sample separation) at a sample bias voltage, V_b , of ~ 200 mV. I-V curves obtained at lower voltages ($V_b = 25$ mV) show no difference in tunneling current between the the two regions (not shown). All I-V curves were obtained using a set-point current of 1.3 nA. At low values of V_b , i.e., 25 mV, the tip to surface separation is reduced, increasing the elastic interaction between the tip and surface. Because both elastic and electronic interactions may contribute to the tunneling current, interpretation of the preliminary TS data on the two crystal structures is not presently possible.

In conclusion, this letter reports STM images of a triangular network of partial dislocations on the (0001) plane of HOPG. Within the stacking fault region bounded by the partial dislocations, a transformation from hexagonal to rhombohedral graphite occurs. STM images in this region show an apparent z-displacement and a difference in the tunneling spectroscopy I-V curves between the faulted and unfaulted regions. This work shows that STM could prove to be a useful tool for characterizing deformation structures on surfaces.

The authors thank Professor John H. Weaver and Dr. Kenneth McGreer for helpful discussions. This work was supported by the Office of Naval Research Young Investigator Program and by the Department of Energy, Basic Sciences Division, Grant DE-FG02-84ER45141. STM facilities were supported by the Center for Interfacial Engineering with funding from NSF Engineering Research Centers Program (CDR 8721551) and industrial sponsors.

Figure Captions

Figure 1. Constant current STM images (a) 2200 nm x 2200 nm and (b) 1000 x 1000 nm (surface plot) of the (0001) plane of HOPG showing an extended network of partial dislocations. Sample bias voltages and tunneling currents were 30 mV and 1.1 nA, respectively.

Figure 2. TEM image of a stacking fault array on the (0001) plane of HOPG (reprinted with permission from 5).

Figure 3. Schematic showing the stacking arrangement in (a) hexagonal graphite, (b) slip transformation from hexagonal to rhombohedral graphite, and (c) rhombohedral graphite.

Figure 4. I vs. V curves taken on a lighter triangle (curve A) and on a darker area (curve B). Sample bias voltage and tunneling current were 200 mV and 1.3 nA, respectively.

References

1. J.M. Soler, A.M. Baro, N. Garcia, and H. Rohrer, Phys. Rev. Lett. **57**(4), 444 (1986).
2. (a) H.J. Mamin, E. Ganz, D.W. Abraham, R.E. Thomson, and J. Clarke, Phys. Rev. B. **34**(12), 9015 (1986), (b) D. Tomanek, S.G. Louie, H.J. Mamin, D.W. Abraham, R.E. Thomson, E. Ganz, and J. Clarke, Phys. Rev. B. **35**(14), 7790 (1987).
3. M. Kuwabara, D.R. Clarke, and D.A. Smith, Appl. Phys. Lett. **56** (24), 2396 (1990).
4. C. Liu, H. Chang, and A.J. Bard, submitted to Langmuir, July 1990.
5. G.K. Williamson, Proc. Roy. Soc. A, **257**, 457 (1960).
6. P. Delavignette and S. Amelinckx, J. Nuclear Materials, **5** (1), 17 (1962).
7. S. Amelinckx and P. Delavignette, J. Appl. Phys., **31** (12), 2126 (1960).
8. H. Lipson and A.R. Stokes, Proc. R. Soc. London, Ser. A, **181**, 101 (1942).
9. S. Fahy, S.G. Louie, and M.L. Cohen, Phys. Rev. B, **34** (2), 1191 (1986).
10. W. Lo, J.C.H. Spence, and M. Kuwabara, STM '90 The Fifth International Conference on Scanning Tunneling Microscopy/Spectroscopy, July 23-27, 1990, Baltimore, Maryland USA.

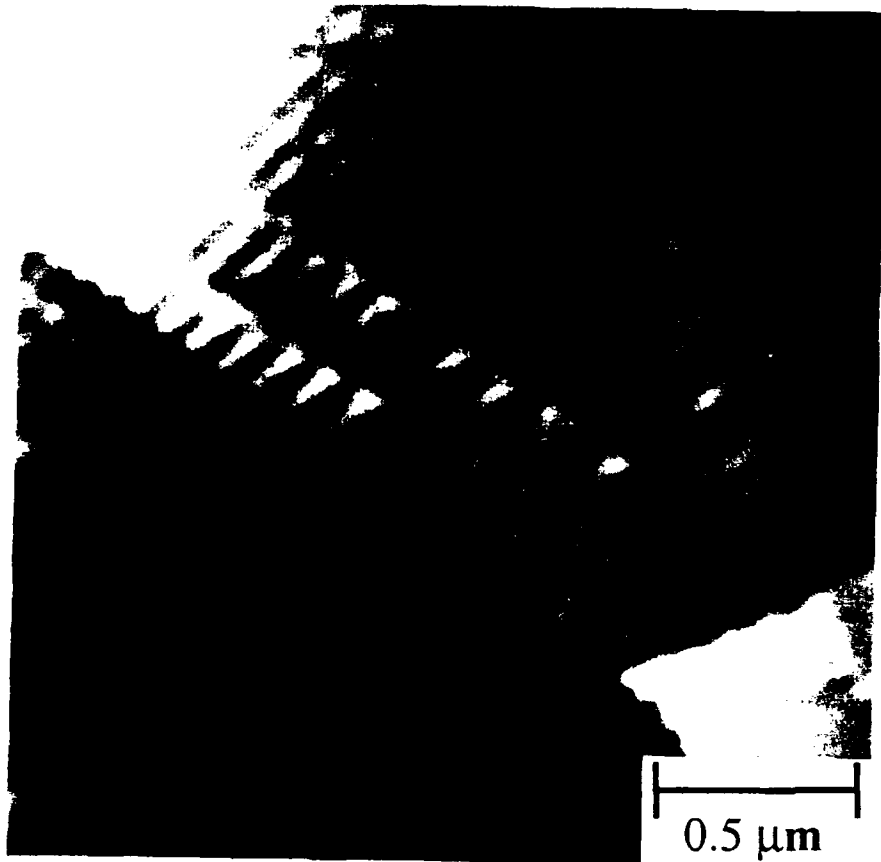


Fig 1(a)

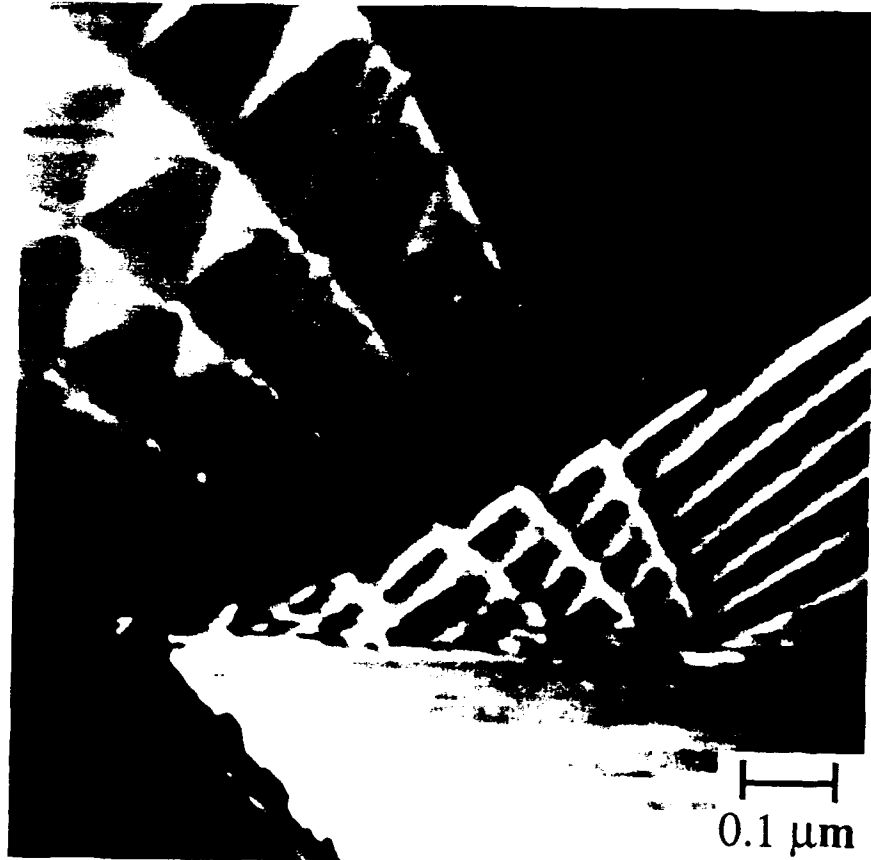
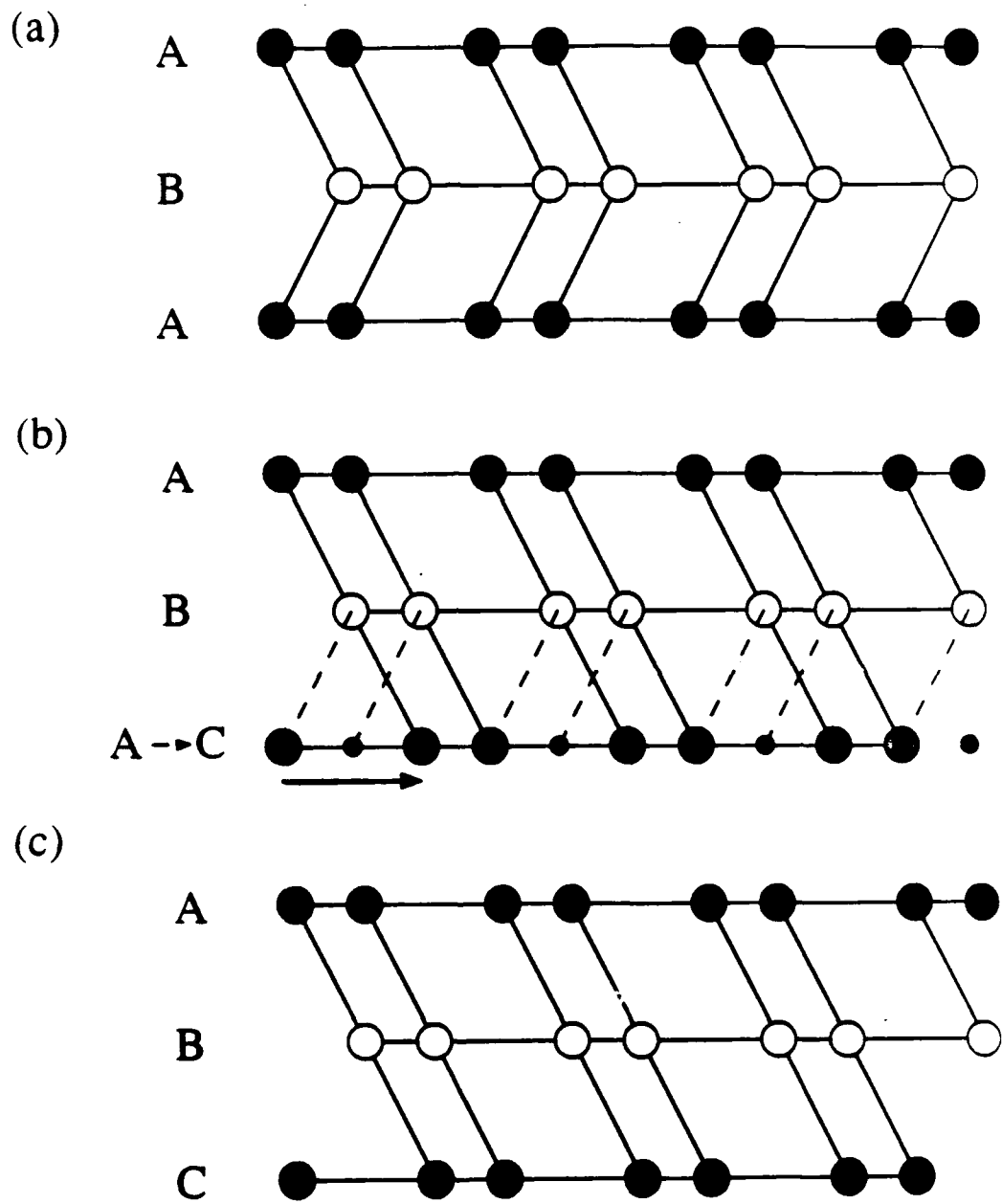


Fig. 1(b)



Fig. 2



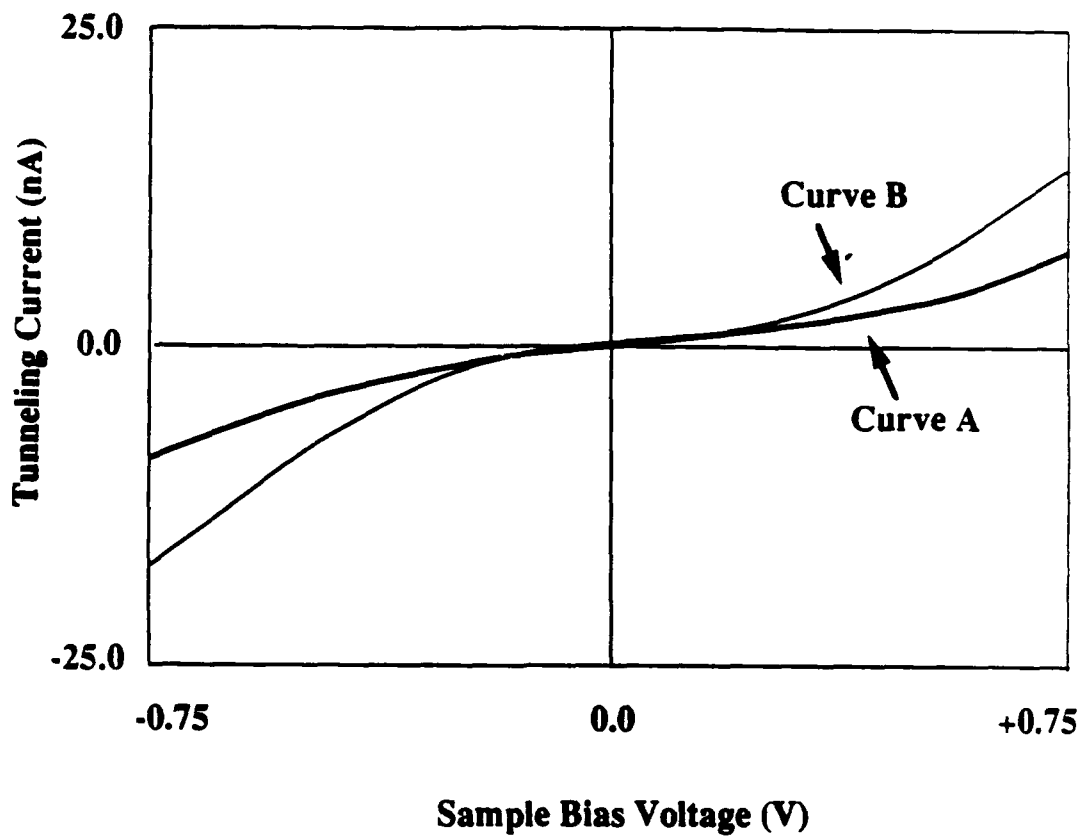


Fig 4